ELSEVIER

Journal of Power Sources 99 (2001) 26–33

JOURNAL OF POWER SOURCES

www.elsevier.com/locate/jpowsour

# Creep characteristics of porous Ni/$Ni_3Al$ anodes for molten carbonate fuel cells

Yun-Sung Kim, Kwan-Young Lee, Hai-Soo Chun*

*Department of Chemical Engineering, Korea University, Seoul 136-701, South Korea*

Received 15 September 2000; accepted 6 December 2000

**Abstract**

The creep behaviour of Ni/(4–7 wt.%) $Ni_3Al$ and Ni/5 wt.% $Ni_3Al$/5 wt.% Cr anodes for molten carbonate fuel cells is classified in terms of two stages during a creep test for 100 h under an applied uniaxial load. The first stage relates to grain rearrangement which results from the destruction of large pores by the applied load. In the second stage, small pores are collapsed by a subsequent sintering process under the load.

The creep resistance of the anodes is enhanced by increasing the sintering resistance through $Ni_3Al$ or $Ni_3Al$ and Cr inclusion, i.e. in comparison with anodes of pure Ni and Ni/10 wt.% Cr. The creep deformation of Ni/5 wt.% $Ni_3Al$/5 wt.% Cr anode is decreased markedly by a synergistic effect of dispersion strengthening and solid-solution strengthening which results from $Ni_3Al$ and Cr addition.


*Keywords:* Creep; Sintering resistance; Anode; $Ni_3Al$; Molten carbonate fuel cell

## 1. Introduction

The molten carbonate fuel cell (MCFC) is a highly efficient and environmentally clean means of power generation. The anode, one of the most important components of the fuel cell, still needs substantial improvement before commercialization of the system can be achieved. In particular, it is essential to determine how to maintain the structural stability of the porous anode under pressurized conditions at elevated temperature [1].

Nickel has been shown to have good electrochemical activity with low polarization loss and, therefore, has been used widely as the anode material for MCFCs for the past two decades. Without strengthening, the porous pure nickel anode would creep significantly during MCFC operation due to the change in pore structure under the compressive stress. In addition, the creep deformation causes the collapse of the stable pore structure, which results in a decrease in the surface area and in the electrochemical performance of the MCFC [2,3]. Therefore, a major research effort has been conducted to strengthen the nickel anode. Partially-sintered Ni anodes dispersed with $Al_2O_3$, Cr or Al particles have been found to exhibit acceptable strength because of dispersion strengthening [4]. Although the creep resistance in these anodes has been improved, the mechanical strength has only been slightly increased.

In our previous studies [1,2], we investigated the sinterability of a porous anode strengthened by Ni–Al intermetallics, especially $Ni_3Al$, and produced by chemical synthesis in an acidic eutectic melt [1,2]. It was found [2,5,6] that the growth of nickel grains in the porous anode strengthened by the inclusion of second-phase particles is retarded during sintering, and a stable open pore network can be maintained by controlling the amount of the included $Ni_3Al$ intermetallics.

In the work reported here, the creep characteristics of Ni/(4–7 wt.%) $Ni_3Al$ and Ni/5 wt.% $Ni_3Al$/5 wt.% Cr anodes, and are investigated and compared with those of pure Ni and Ni/10 wt.% Cr anodes in terms of microstructure.

## 2. Experimental

A creep experiment was performed on samples (1 cm × 1 cm) fabricated from pure Ni, Ni/(4–7 wt.%) $Ni_3Al$, Ni/5 wt.% $Ni_3Al$/5 wt.% Cr and Ni/10 wt.% Cr anodes which were sintered to the same porosity, viz. 62% [2,7].

* Corresponding author. Tel.: +82-2-3290-3292; fax: +82-2-9266-102.
*E-mail address*: hschun@mail.korea.ac.kr (H.-S. Chun).

0378-7753/01/$ – see front matter 
PII: S0378-7753(00)00689-3

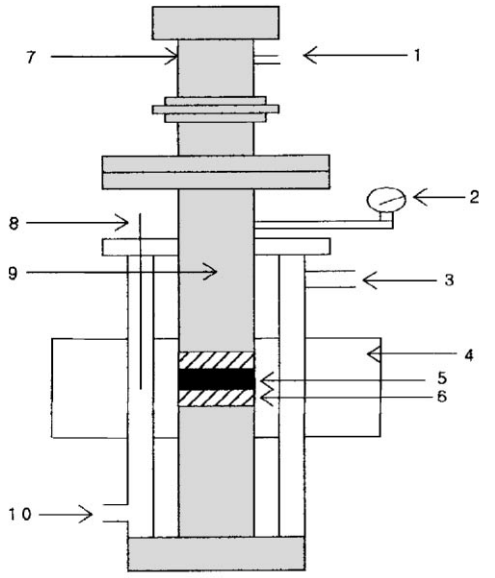


Fig. 1. Schematic diagram of creep test apparatus.

The samples were first placed in the creep test apparatus, as shown in Fig. 1. The furnace was heated at a rate of 100°C/h, and temperature was then maintained at 650°C; the maximum temperature error was ±0.5°C during the experiment. A gas mixture of 70% $H_2/CO_2$ was passed through the furnace at a rate of 100 ml/min. An external load of 100 psi was transmitted to samples by means of a pressure rod driven by an air cylinder. In a separate set of experiments, the test was terminated after times between 0 and 100 h.

The dimensions of the samples were measured with a micrometer before and after the creep test, and the pore-size distributions were obtained by means of mercury porosimetry (Micrometrics Autopore II 9215). The fracture and surface of the sample before and after the test were examined with a scanning electron microscope (Jeol JSM-5200). To obtain the mechanical strength of the porous anodes, the tensile strength was measured with a universal test machine (Instron UTM 4467).

## 3. Results and discussion

Creep rates for the anodes are shown in Fig. 2. The rates were obtained from creep strain curves measured during a constant uniaxial pressure of 100 psi for 100 h. Clearly, the compressive load has a systematic and pronounced effect on creep behaviour. The creep rates of anodes with $Ni_3Al$ quickly reach a steady-state compared with that of the pure Ni anode; the rates remain constant after about 60 h. Also,

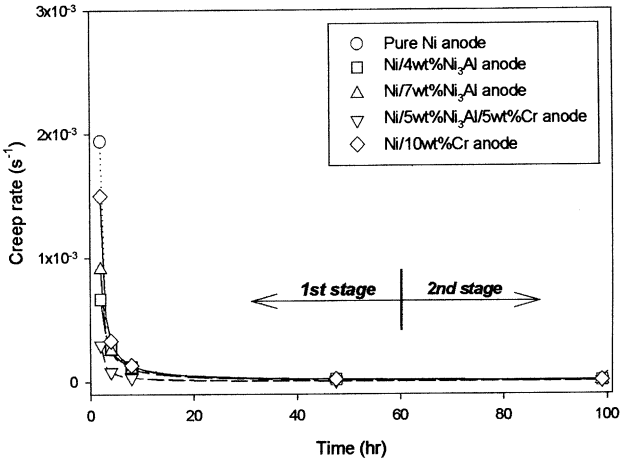


Fig. 2. Creep rate curves for porous anodes obtained from creep tests with a constant uniaxial load of 100 psi for 100 h.

the creep deformation of the anodes appears to decrease with an increasing amount of $Ni_3Al$. In particular, the creep rate of the Ni/5 wt.% $Ni_3Al$/5 wt.% Cr anode is considerably lower than that of the other anodes.

The creep behaviour of these porous anodes consists of two stages. This is different from that observed for high-density polycrystalline materials which is generally composed of three stages. The first stage, during which (possibly after an instantaneous load) the creep rate decreases rapidly with time, is related to a change in the pore structure of the anodes. The creep rate of the pure Ni anode decreases faster than the rates of other anodes; the latter rates show little change after 8 h. The creep rates of all the anodes are almost time-invariant after 60 h. This is taken to be the second stage and is analogous to steady-state creep or secondary creep of the high-density material.

The relationships between the creep rate and the creep strain for the anodes are presented in Fig. 3. The creep rate and the creep strain of the Ni/5 wt.% $Ni_3Al$/5 wt.% Cr anode

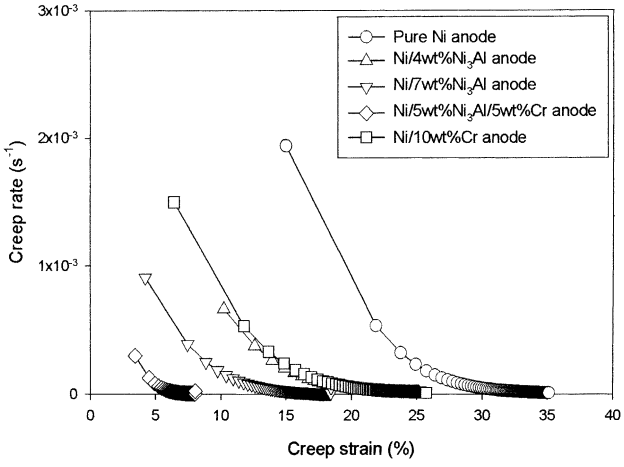


Fig. 3. Relationship between creep rate and creep strain for porous anodes.

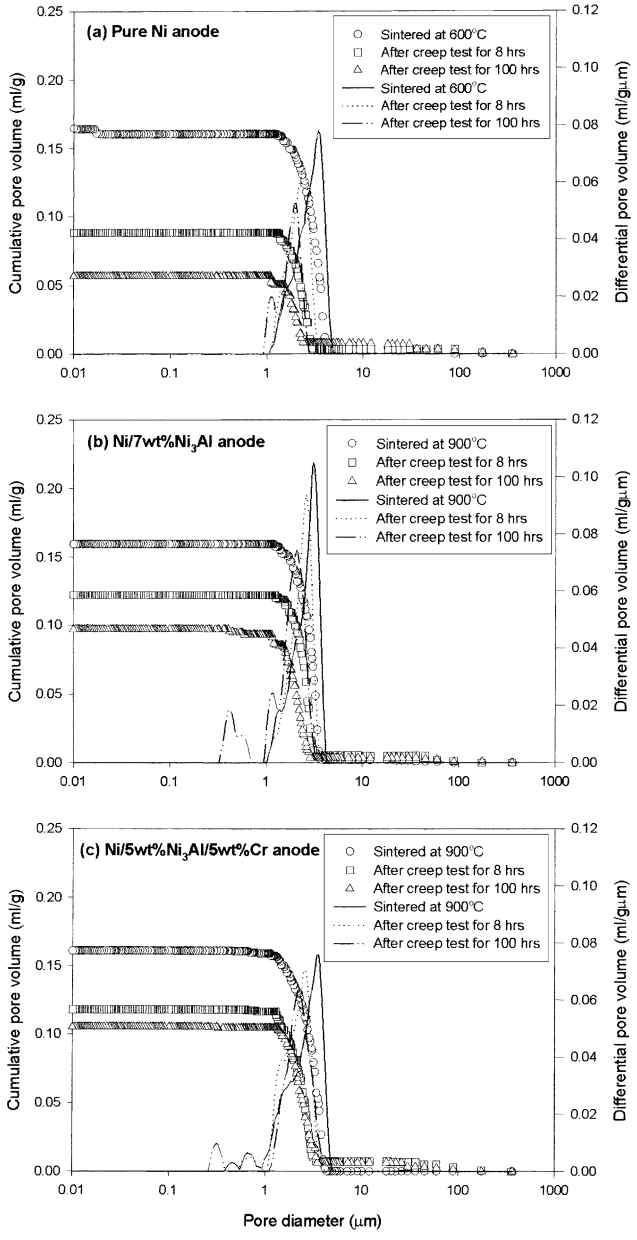


Fig. 4. Pore-size distribution curves of porous anodes before and after creep test.

under a constant load are relatively lower than those of Ni/7 wt.% $Ni_3Al$ anodes strengthened only by $Ni_3Al$ inclusion.

Pore-size distribution curves for the anodes sintered to the same porosity, viz. 62%, before and after the creep test are presented in Fig. 4. The porosity of the anodes is controlled by a sintering condition of their green sheet [2]. Large pores (3–5 μm) of the pure Ni anode are collapsed by the applied load after an interval of 8 h in the first stage, and the pore structure is deformed continuously even in the second stage. On the other hand, the pores in Ni/7 wt.% $Ni_3Al$ and Ni/5 wt.% $Ni_3Al$/5 wt.% Cr anodes maintain a relatively stable porous structure after 100 h of the creep test during; there is a slight collapse of the pore structures in the first stage.

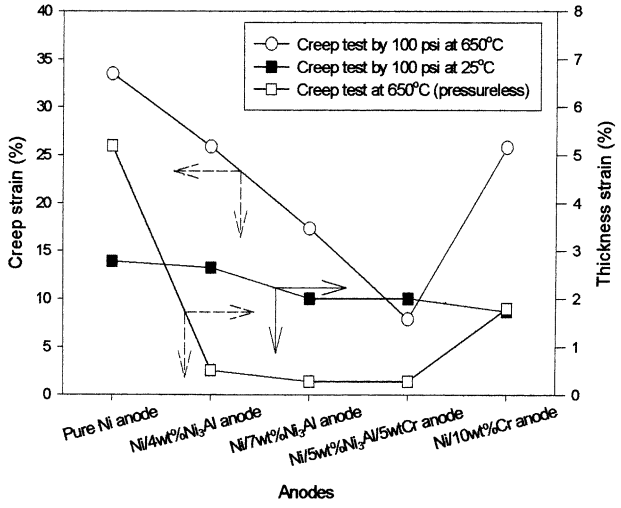


Fig. 5. Creep and thickness strain for porous anodes under different test conditions.

The effects of compressive load and temperature on the creep strain of the anodes are shown in Fig. 5. The thickness strain for anodes with $Ni_3Al$ or with $Ni_3Al$ and Cr inclusion exerted by the applied load of 100 psi at room temperature after the creep test during 100 h is considerably higher than that obtained in an incompressive creep experiment at 650°C, except for the pure and Ni/10 wt.% Cr anodes. Because creep deformation of porous anodes is generally influenced by the sintering shrinkage rather than by the applied load, $Ni_3Al$ inclusion increases the sintering resistance due to inhibition of the growth of nickel grains [1]. Therefore, it is concluded from these experiments that sintering resistance is one of the most important factors in increasing the creep resistance of the porous anode. In particular, the Ni/5 wt.% $Ni_3Al$/5 wt.% Cr anode has a higher creep resistance than any of the other anodes. It is considered that the creep resistance of porous anodes with $Ni_3Al$ inclusion can be increased by a synergistic effect of dispersion strengthening and solid-solution strengthening.

The morphology of the cracks and the surfaces of pure Ni, Ni/7 wt.% $Ni_3Al$ and Ni/5 wt.% $Ni_3Al$/5 wt.% Cr anodes with the same porosity before and after creep test, are shown by the scanning electron micrographs in Figs. 6–8, respectively. For the pure Ni anode, the curvature of the neck between the nickel grains is decreased, and the grain grows by vigorous mass transport [2]. Neither grain growth nor crack propagation is observed in the surface and the fracture of Ni/7 wt.% $Ni_3Al$ and Ni/5 wt.% $Ni_3Al$/5 wt.% Cr anodes. Creep deformation in the Ni/5 wt.% $Ni_3Al$/5 wt.% Cr anode results from deformation of the pore structure by the load rather than by sintering.

A porous compact formed by various powder processing methods develops complex states of internal stress with progress of a sintering process. This effect is due partially to the so-called sintering stress which acts locally at the

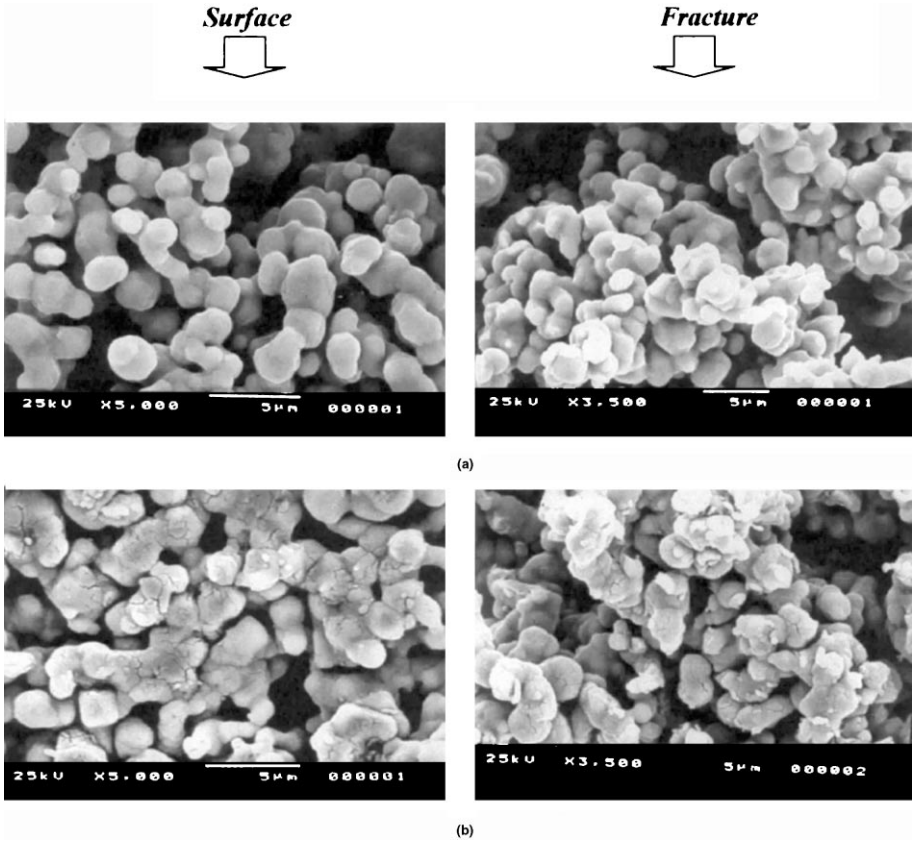


Fig. 6. Electron micrographs of pure Ni anode: (a) before and (b) after creep test.

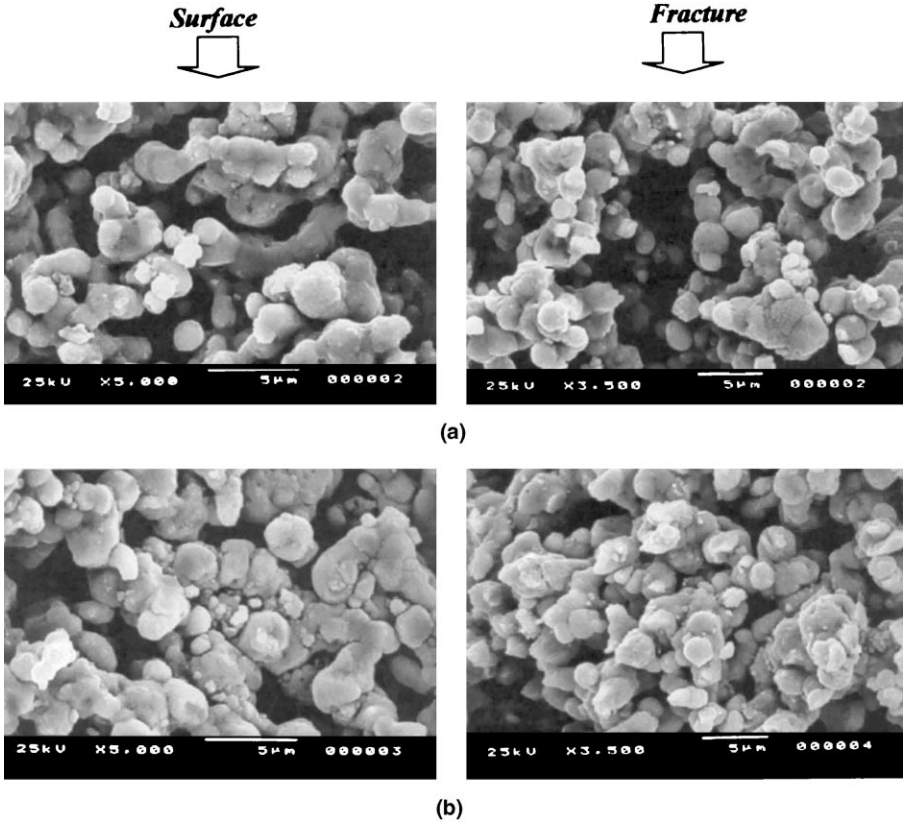


Fig. 7. Electron micrographs of Ni/7 wt.% $Ni_3Al$ anode: (a) before and (b) after creep test.

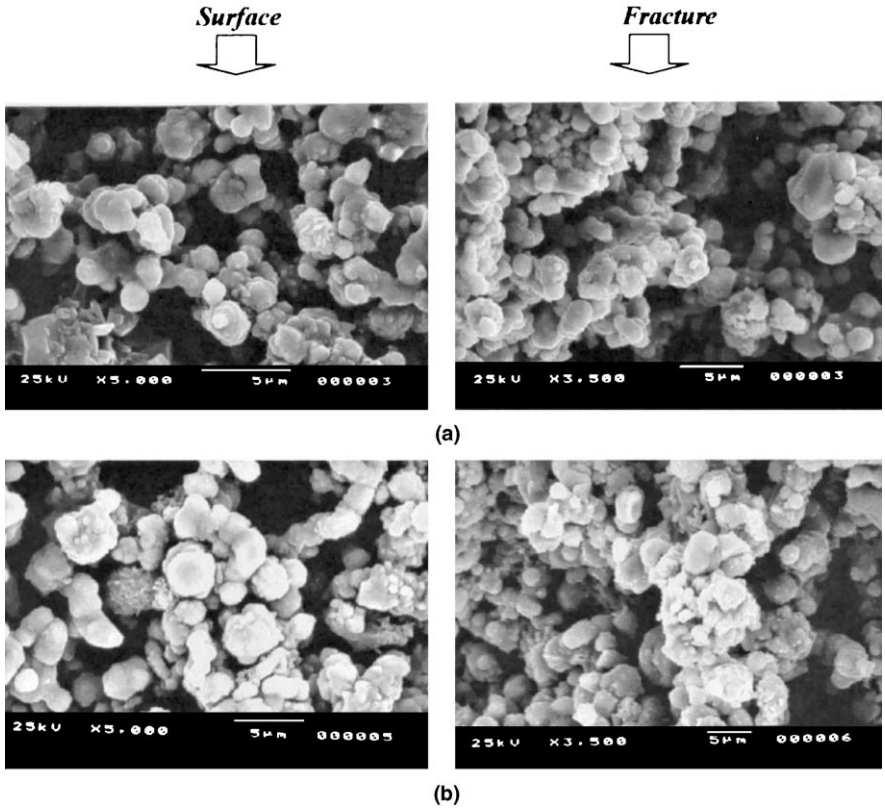


Fig. 8. Election micrographs of Ni/5 wt.% $Ni_3Al$/5 wt.% Cr anode: (a) before and (b) after creep test.

joints between individual grains and partially to the external load [8].

These stresses tend to concentrate in the neck cross-sections and can be expressed, at a given instant of the process, by a simplified topological network in which knots represent the grain centres and each bar is the bond between a two given grains, as shown in Fig. 9. If the grains are uniform in size and closely packed, the dominant action is normal stress, while bending moments are negligible. Such a situation is typical of high-density porous materials. With highly porous materials, the network is largely defective and the effect of bending moments becomes important.

In general, a green sheet for a MCFC is a porous compact of mechanically interlocked grains where no rearrangement of the grains is possible under the action of a weak applied stress. At the sintering temperature, neck formation starts from the contact regions of the grains and these then grow into grain boundary interfaces. Therefore, a stress gradient in the network of highly porous materials will produce a net diffusional flow of matter in the stressed domain of the joint, i.e. from more compressive regions towards less compressive regions. Thus, the grains undergo a deformation which is concentrated in the region of the neck and which, if allowed by the geometry, will result in a reciprocal tilt or sliding as determined by the dominant creep mechanism.

If the shape of the grain is at least approximately conserved, as is the case during the initial stage of sintering, movement of the grain aggregate can be described simply in terms of a tilt angle, as shown in Fig. 10 [8].

While creep deformation in the high-density material proceeds mainly by growth of the necks between grains and is accelerated by surface diffusion or grain boundary diffusion under the applied compressive stress, analysis of the creep behaviour of highly porous material must consider deformation caused by the bending moment as well as by the compressive stress. Local movement in the latter material will give rise to a global rearrangement of the grain network in which large pores will collapse substantially, to cause large changes in shape. It is considered, therefore, that the creep mechanism of porous anodes for MCFCs can be divided into two stages from the viewpoint of microstructure. Grain rearrangement corresponds to the first stage, in which large pores are collapsed by the rearrangement of the grains to stable sites due to the compressive stress and the bending moment exerted in the vicinity of the neck; large pores are virtually destroyed during this stage. In the second stage, small pores are diminished by the sintering stress due to mass transport accelerated under the applied stresses.

For the pure Ni anode, most of the large pores are rapidly collapsed by grain rearrangement during 8 h, and the deformation continues during the second stage, as shown in Fig. 4(a). The porosity is decreased to 45% after 100 h of the creep test and the pore structure is considerably collapsed. On the other hand, the creep behaviour of Ni/4–7 wt.%

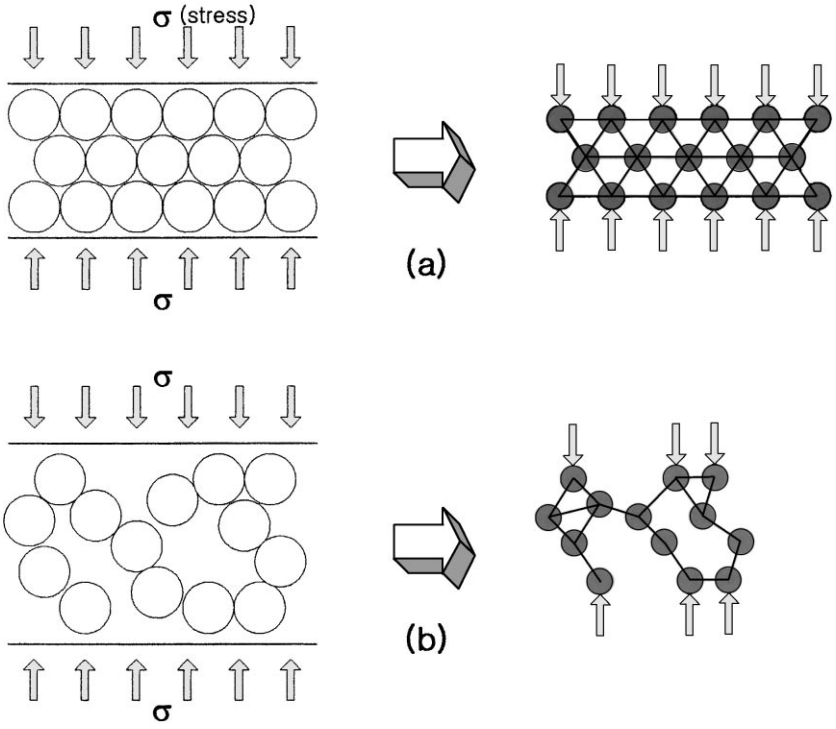


Fig. 9. Network representation of neck between grains of (a) closed-packed and (b) highly porous grain aggregates [8].

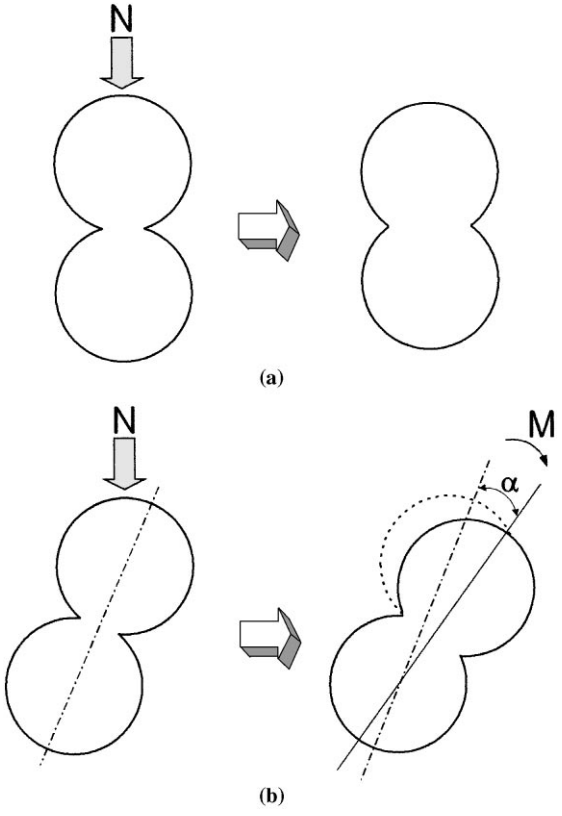


Fig. 10. Creep behavior by (a) neck growth due to mass transport and (b) grain rearrangement (N: compressive stress; M: bending stress) [8].

$Ni_3Al$ and the Ni/5 wt.% $Ni_3Al$/5 wt.% Cr anodes is restricted to the first stage, and the deformation is mainly caused by the applied load rather than by sintering shrinkage. In addition, the pore structures maintain stable open networks by inhibition of the growth of the nickel grains due to $Ni_3Al$ inclusion, as shown in Fig. 4(b) and (c).

The tensile strength and the Young's modulus of the anodes are presented in Fig. 11 (measured by the universal test machine (UTM)). The mechanical strength of the Ni/5 wt.% $Ni_3Al$/5 wt.% Cr anode is considerably higher than that of any of the other anodes, and results from a synergistic effect of dispersion strengthening and solid-solution strengthening by the $Ni_3Al$ and Cr. Strength tests show that higher tensile strength of the porous anode results in higher creep resistance.

Electron micrographs of a fracture in the anodes tested by the UTM are given in Fig. 12. To maintain the porosity at 62%, sintering of these anodes is controlled within temperatures which range from 600 to 900°C by different mass transport mechanisms between the nickel grains [2]. The fracture of the pure Ni anode is relatively smoother than that of other anodes, and the nickel grains of the fracture surface of Ni/10 wt.% Cr anode are elongated by solid-solution strengthening due to Cr addition. On the other hand, the mechanical strength during tensile stress of the Ni anode strengthened by $Ni_3Al$ or $Ni_3Al$ and Cr inclusion can be considerably increased due to strong bonding between small nickel grains.

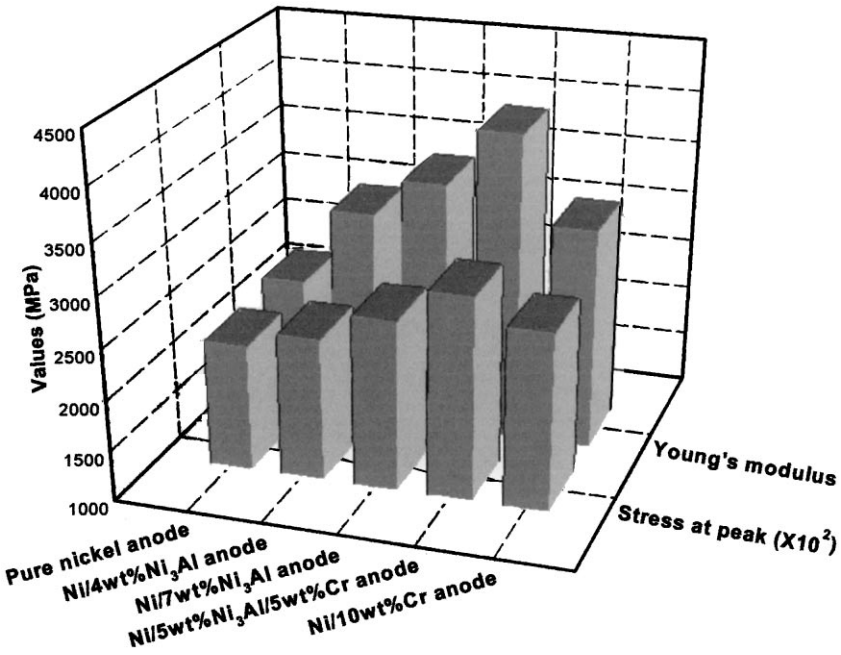


Fig. 11. Mechanical properties of MCFC anodes measured with the universal test machine.

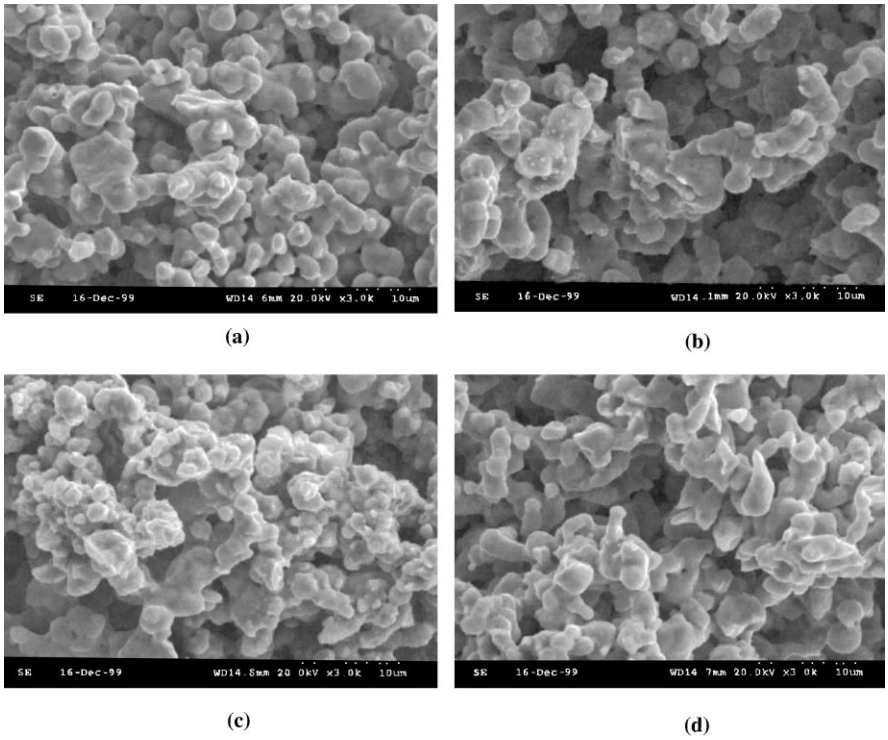


Fig. 12. Electron micrographs of fracture of (a) pure Ni; (b) Ni/7 wt.% $Ni_3Al$; (c) Ni/5 wt.% $Ni_3Al$/5 wt.% Cr and (d) Ni/10 wt.% Cr anodes after tensile strength test.

## 4. Conclusions

Creep behaviour of Ni/(4–7 wt.%) $Ni_3Al$ and Ni/5 wt.% $Ni_3Al$/5 wt.% Cr anodes for MCFCs is composed of two stages. In the first stage, nickel grains rearrange to a stable site in the porous structure after most of the large pores have collapsed under the applied load. In the second stage, small pores are shrunk by the sintering process which is

accelerated under the applied load. It is also found that the creep resistance of the porous anodes is enhanced by increasing the sintering resistance through $Ni_3Al$ or $Ni_3Al$ and Cr inclusion. In particular, the creep deformation of Ni/5 wt.% $Ni_3Al$/5 wt.% Cr is decreased considerably by a synergistic effect of dispersion strengthening and solid-solution strengthening by the addition of $Ni_3Al$ and Cr.

## Acknowledgements

This work was supported in part by a Korea Research Foundation Grant (KRF-99-042-E00075).

## References

[1] Y.S. Kim, S.I. Lee, J.H. Lim, H.S. Chun, J. Chem. Eng. Jpn. 33 (2000) 96.
[2] Y.S. Kim, H.S. Chun, J. Power Sources 84 (1999) 80.
[3] J.H. Lim, Y.S. Kim, H.S. Chun, J. Corros. Sci. Soc. Korea 28 (1999) 381.
[4] C. Yuh, R. Johnsen, M. Farooque, H. Maru, J. Power Sources 62 (1995) 1.
[5] Y.S. Kim, H.S. Choo, M.C. Shin, M.Z. Hong, J.H. Lim, H.S. Chun, in: Proceedings of the 3rd International Fuel Cell Conference, NEDO/NITI, Nagoya, Japan, 1999, p. 417.
[6] J.H. Lim, Y.S. Kim, H.S. Choo, M.C. Shin, S.I. Lee, H.S. Chun, in: Proceedings of the 3rd International Fuel Cell Conference, NEDO/NITI, Nagoya, Japan, 1999, p. 413.
[7] H.S. Choo, M.S. Thesis, Korea University, Seoul, South Korea, 2000.
[8] D. Beruto, M. Capurro, R. Botter, J. Mater. Sci. 30 (1995) 4994.